



ARCHIVIO ISTITUZIONALE DELLA RICERCA

Alma Mater Studiorum Università di Bologna Archivio istituzionale della ricerca

Cor triatriatum sinister in a dog

This is the final peer-reviewed author's accepted manuscript (postprint) of the following publication:

Published Version:

Cor triatriatum sinister in a dog / Castagna P.; Romito G.; Baron Toaldo M.. - In: JOURNAL OF VETERINARY CARDIOLOGY. - ISSN 1760-2734. - ELETTRONICO. - 25:(2019), pp. 25-31. [10.1016/j.jvc.2019.07.003]

This version is available at: <https://hdl.handle.net/11585/720693> since: 2020-02-03

Published:

DOI: <http://doi.org/10.1016/j.jvc.2019.07.003>

Terms of use:

Some rights reserved. The terms and conditions for the reuse of this version of the manuscript are specified in the publishing policy. For all terms of use and more information see the publisher's website.

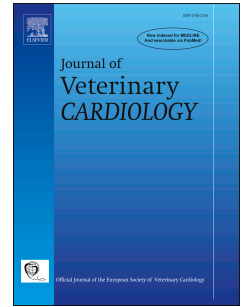
(Article begins on next page)

This item was downloaded from IRIS Università di Bologna (<https://cris.unibo.it/>).
When citing, please refer to the published version.

Accepted Manuscript

Cor triatriatum sinister in a dog

Prisca Castagna, DVM, Giovanni Romito, DVM, PhD, Marco Baron Toaldo, DVM, PhD



PII: S1760-2734(18)30210-8

DOI: <https://doi.org/10.1016/j.jvc.2019.07.003>

Reference: JVC 589

To appear in: *Journal of Veterinary Cardiology*

Received Date: 14 December 2018

Revised Date: 25 June 2019

Accepted Date: 18 July 2019

Please cite this article as: Castagna P, Romito G, Toaldo MB, Cor triatriatum sinister in a dog, *Journal of Veterinary Cardiology*, <https://doi.org/10.1016/j.jvc.2019.07.003>.

This is a PDF file of an unedited manuscript that has been accepted for publication. As a service to our customers we are providing this early version of the manuscript. The manuscript will undergo copyediting, typesetting, and review of the resulting proof before it is published in its final form. Please note that during the production process errors may be discovered which could affect the content, and all legal disclaimers that apply to the journal pertain.

1 **Cor triatriatum sinister in a dog**

2 Prisca Castagna, DVM, Giovanni Romito, DVM, PhD, Marco Baron Toaldo, DVM, PhD

3
4 Department of Veterinary Medical Sciences, Alma Mater Studiorum - University of
5 Bologna, Italy.

6
7 This work was done at the Department of Veterinary Medical Sciences, Alma Mater
8 Studiorum - University of Bologna, Via Tolara di Sopra 50, 40064 Ozzano Emilia, Italy.

9
10 Corresponding author: M Baron Toaldo, E-mail marco.barontoaldo@unibo.it

11
12
13 **Short title:** Cor triatriatum sinister

14 **Abstract**

15 This report describes the transthoracic and transesophageal echocardiographic features
 16 of a *cor triatriatum sinister* in an asymptomatic 6-year-old male French bulldog. Although
 17 *cor triatriatum sinister* represents a well-known and widely described cardiac
 18 malformation in humans, its description in the canine population is rare. In this clinical
 19 case, non-invasive echocardiographic techniques were helpful in visualizing and
 20 characterizing the lesion, allowing a valuable assessment of the malformation, and its
 21 hemodynamic consequences.

22

23 **Abbreviation Table**

AC	accessory atrial chamber
CTS	cor triatriatum sinister
LA	left atrium
LV	left ventricle
TEE	transesophageal echocardiography
TTE	transthoracic echocardiography

24

25 **Keywords**

26 Transesophageal echocardiography; cardiac malformation; left atrium; canine.

27

28 **Introduction**

29 A 6-year-old, male intact, French bulldog weighing 14 kg was referred to the
30 Veterinary Teaching Hospital of the University of Bologna for surgical resection of a low-
31 grade cutaneous mast cell tumor. The dog appeared otherwise healthy. Specifically,
32 cardiac auscultation revealed a regular rhythm with a heart rate of 136 beats/minute; no
33 heart murmur could be detected. Femoral pulse quality was good and the examination of
34 jugular veins showed no abnormalities. Thoracic radiographs were obtained as part of
35 neoplastic disease staging.

36

37 **Image interpretation:**

38 **Figure 1. Thoracic radiography**

39 Survey radiographic study of the thorax of a French Bulldog, obtained in two
40 perpendicular projections. On left lateral recumbency (Fig. 1A) a deformation of the left
41 atrial (LA) profile is evident (white dotted line). No other alterations of the cardiac
42 silhouette were noticeable in ventrodorsal projection (Fig. 1B). Given the radiographic LA
43 abnormality, pre-anesthetic echocardiography was recommended. Complete
44 transthoracic echocardiography (TTE), including two-dimensional, M-Mode, and Doppler
45 analysis, was performed according to a standard technique [1] using an ultrasound unit^a
46 equipped with multi-frequency phased array transducers and with continuous ECG
47 monitoring.

48

49 **Figure 2 and Video 1. Two-dimensional transthoracic echocardiography**

50 On right parasternal long axis view (Fig. 2A, Video 1), the atrioventricular valves were
51 morphologically normal as well as the left ventricular (LV) dimensions and systolic
52 function. Within the LA, an interrupted linear hyperechoic structure compatible with a
53 fenestrated membrane was identified. This anomalous membrane appeared to transect
54 the LA partitioning it into two discrete chambers. The proximal portion (the accessory
55 atrial chamber [AC]) appeared located dorso-caudally, while the distal portion (the true
56 LA) was in direct communication with the LV, through the mitral valve orifice, and
57 contained the atrial septum. Some pulmonary veins were draining into the AC (star),
58 while others were connected to the true LA (asterisks). The region of the *fossa ovalis*
59 appeared particularly thin but intact based on Color Doppler interrogation on TTE. The
60 short axis view at the level of the cardiac base (Fig. 2B) provided a better visualization of
61 the AC and its direct connection to some pulmonary veins (white stars). The left auricle
62 was, instead, part of the true LA. Combining information obtained from both
63 echocardiographic views, the right middle lobe and the right cranial lobe pulmonary veins
64 were judged to drain into the LA, while the AC appeared to receive the blood from the left
65 caudal and left cranial lung lobes, the accessory lobe and the right caudal lobe
66 pulmonary veins [2]. Computed tomography was not performed to further characterize
67 the pulmonary venous drainage.

68

69 **Video 2. Color Doppler transthoracic echocardiography**

70 On Color Doppler analysis obtained through a left apical four-chamber view, a
71 continuous forward blood flow across the membrane's orifice was evident. The true LA

72 was receiving blood coming from both the AC, with a turbulent jet directed toward the
73 anterior mitral valve leaflet, and the pulmonary veins likely draining the right cranial and
74 middle lung lobes. The remainder of the echocardiographic study was normal. In light of
75 the above-mentioned findings, a *cor triatriatum sinister* (CTS) was diagnosed.

76 One week after the TTE, the surgical resection of the cutaneous mast cell tumor was
77 performed without any complications. Immediately after surgery, still under general
78 anesthesia, transesophageal echocardiography (TEE) was carried out using a dedicated
79 probe^b, to better characterize the cardiac malformation.

80

81 **Figure 3, Video 3. Transesophageal echocardiography – Two-dimensional and**
82 **Color Doppler analysis**

83 Transesophageal echocardiography was performed with the dog positioned in
84 right lateral recumbency following standard techniques [3]. Figure 3A shows a middle
85 position TEE view, with the cursor angle set at 141°, obtaining a modified four-chambers
86 view. The AC is visible on the upper right part of the image with the perforated
87 membrane identified by the star. The interatrial septum was normal in appearance. A
88 slight rotation of the cursor to 116°, allowed visualization of the LV outflow tract and
89 aorta (Fig. 3B, Video 3). Color Doppler analysis clearly showed a continuous turbulent
90 blood flow across the membrane's orifice directed straight toward the anterior mitral
91 valve leaflet. Additionally, a mild systolic mitral valve regurgitation was evident and
92 eccentrically directed.

93

94 **Figure 4. Transesophageal echocardiography – Spectral Doppler and color M-**
95 **Mode analysis**

96 The continuous-wave Doppler analysis of the transmembrane blood flow revealed
97 a continuous systo-diastolic flow with a maximal velocity during ventricular diastole
98 (velocity 1.8 m/s; pressure gradient 13 mmHg) and a minimal velocity during ventricular
99 systole (velocity 1.3 m/s; pressure gradient 7 mmHg). A short notch on the spectral
100 profile occurred in concomitance with mitral valve closure (Fig. 4A). The maximal
101 pressure into the AC was estimated to be around 20 mmHg, assuming a LA systolic
102 pressure of 7–8 mmHg.

103 The Color Doppler and the M-Mode modalities were combined to display
104 mechanical events in addition to flow events simultaneously in the AC, LA, and LV (Fig.
105 4B). The cursor line was superimposed to the turbulent jet; therefore, on the M-Mode
106 trace, the LA tier was occupied by an aliased/mainly yellow colored flow. The movement
107 of the anterior mitral valve leaflet set the passage of blood into the LV that filled during
108 early and late diastolic phase (blue bands in the bottom tier). The red jet represented a
109 mild early systolic mitral valve regurgitant jet (arrowhead). The narrow blue band
110 between the AC and the LA tiers reflected the small area of isovelocity of the turbulent
111 jet on the AC side of the perforated membrane.

112 After completion of the TEE, the dog recovered uneventfully from anesthesia and
113 was discharged on the same day. No therapies were recommended for the cardiac
114 abnormality, but echocardiographic rechecks were suggested to monitor the
115 malformation over time.

116

117 **Discussion**

118 *Cor triatriatum sinister* is a rare cardiac malformation in which the LA is divided
119 into two compartments by an anomalous membrane. Consequently, three atrial
120 chambers can be identified: the right atrium, the actual true LA, and the AC connected to
121 the LA (hence the term '*triatriatum*') [5]. The membrane that transects LA varies
122 significantly in size and shape; it may appear similar to a diaphragm or be funnel-
123 shaped, entirely intact (imperforate), or contain one or more fenestrations with different
124 diameters [5]. In humans, CTS represents only 0.1–0.4% of all congenital cardiac
125 malformations and may be associated with other cardiac defects in as many as 50% of
126 cases, especially atrial septal defects and abnormalities of the pulmonary venous return
127 [5]. As opposed to the more frequently described *cor triatriatum dexter* in dogs and CTS
128 in cats, CTS is rare in the canine species. Thus far, only two cases have been
129 published, both presented as a solitary malformation associated with signs of congestive
130 heart failure [6,7]. Specifically, in one case (a 3-year-old male French Bulldog) the
131 diagnosis was made exclusively by TTE when clinical signs of lung edema developed
132 [6], while in the other one (a 5-year-old female Poodle) evidence of CTS was obtained
133 exclusively by post-mortem examination [7]. Although several theories have been
134 hypothesized in human medicine, the embryologic basis of CTS is still a controversial
135 subject. To date three main theories have been proposed: the “malincorporation”
136 (incomplete incorporation of the common pulmonary vein into the LA), the “malseptation”
137 (the septum subdividing the left atrium is the result of an abnormal overgrowth of *septum*
138 *primum*), and the “entrapment” (the left horn of the embryonic *sinus venosus* entraps the

139 common pulmonary vein; thereby, preventing its incorporation into the LA) [5]. In
140 humans, several classifications of CTS have been suggested based on the
141 communication between the AC and the other cardiac chambers, the quantity and
142 morphology of fenestrations of the anomalous membrane, and concurrent anomalies of
143 the venous return [8]. According to the classification proposed by Krabill and Lucas,
144 1995 [9], the dog of this report had a CTS with a C1A morphology, characterized by a
145 subtotal CTS where the AC connects to the LA and receives part of the pulmonary
146 veins, while the remaining pulmonary veins drain normally into the true LA. Human and
147 canine patients with CTS may be asymptomatic, as in the case presented here, or show
148 signs of left-sided congestive heart failure due to the obstruction to the flow between the
149 pulmonary venous system and the left ventricle [5-7]. The development of clinical signs
150 and the time of their occurrence mainly depends on the size and number of the
151 fenestrations in the membrane as well as the presence of concurrent heart abnormalities
152 [5]. In human medicine, several imaging techniques have been used to establish the
153 CTS diagnosis, including two-dimensional as well as three-dimensional TTE and TEE,
154 cardiac catheterization and selective angiography, computed tomography, and magnetic
155 resonance imaging [8]. Traditionally, either in human and veterinary medicine, TTE has
156 represented the first line diagnostic modality, because it is relatively inexpensive, widely
157 available, non-invasive, and easy to perform. Additionally, this imaging technique can
158 identify the possible hemodynamic compromise associated with the CTS and it might
159 reveal concomitant cardiac abnormalities [6-8]. In cases of CTS associated with multiple
160 cardiac defects or for patients with a peculiar chest conformation (e.g., obese human
161 patients, brachycephalic canine breeds), TTE alone could lead to an inadequate
162 visualization of the AC and of the abnormal membrane. In such cases, TEE has been

163 demonstrated to represent a valuable complementary tool in people [8]. As compared
164 with TTE, TEE offers superior visualization of cardiac structures because of the close
165 proximity of the esophagus to the heart and lack of superimposition of the lungs,
166 muscles, and bones. Additionally, this proximity permits use of high-frequency imaging
167 transducers that afford superior spatial resolution [3]. In the case described here, TEE
168 allowed a better visualization of the LA anatomy, of the interatrial septum, and the
169 abnormal membrane, with confirmation of the malformation and of the origin of the
170 pathologic flow.

171 In symptomatic human patients, medical therapy can be initially set up to control
172 the clinical signs of congestive heart failure, although the treatment of choice remains
173 the surgical resection of the intra-atrial membrane [5]. Alternatively, minimally invasive
174 per-catheter balloon dilatation of the membrane can be considered [10]. To date, only
175 the medical approach (e.g., furosemide, benazepril) has been reported in canine CTS
176 [6-7], although either surgical resection and balloon dilation have been demonstrated to
177 be effective in dogs with *cor triatriatum dexter* [11] and in cats with CTS [12]. Among the
178 two therapeutic options, balloon dilation represents a less expensive and dangerous
179 approach for this malformation in small animals [13]. A hybrid technique, performed by
180 inserting an inflatable balloon through the defect after thoracotomic approach to the LA,
181 has also been successfully performed in one cat with CTS [14]. In asymptomatic human
182 patients, no intervention is usually advised but regular rechecks are planned over time to
183 identify any progressive narrowing of the membrane's orifice, signs of venous
184 congestion, or occurrence of pulmonary hypertension. In the dog from the present
185 report, the elected approach was to monitor given that the patient was asymptomatic

186 and there was no evidence of pulmonary venous congestion. On the other side the
187 measured gradient across the membrane was about 20 mmHg. It might be speculated
188 that this chronic increase in pressure might lead to a remodeling of the affected
189 vasculature, and possibly induce a chronic and clinically relevant pulmonary
190 hypertension. Considering the overall case a “wait and see” approach was considered
191 more appropriate, and an interventional treatment was offered as a plausible option in
192 case the malformation became hemodynamically relevant.

193 In conclusion, this is the first report of a canine CTS extensively described with
194 the use of TTE and TEE. The addition of another imaging modality such as TEE may
195 help to further expand the characterization of this rare congenital defect.

196

197 **Conflict of interest**

198 The authors do not have any conflicts of interest to declare.

199

200 **Funding**

201 This research received no grant from any funding agency in the public, commercial or
202 not-for-profit sectors.

203 **Footnotes**

204 ^a iE33 ultrasound system, Philips Healthcare, Monza, Italy.

205 ^b X7-2t transesophageal phased array transducer, Philips Healthcare, Monza, Italy

206

207 **References**

208 [1] Thomas WP, Gaber CE, Jacobs GJ, Kaplan PM, Lombard CW, Moise NS, Moses
209 BL. Recommendations for standards in transthoracic two-dimensional echocardiography
210 in the dog and cat. Echocardiography Committee of the Specialty of Cardiology,
211 American College of Veterinary Internal Medicine. J Vet Intern Med 1993;7:247-52.

212 [2] Brewer FC, Moïse NS, Kornreich BG, Bezuidenhout AJ. Use of computed
213 tomography and silicon endocasts to identify pulmonary veins with echocardiography. J
214 Vet Cardiol 2012;14:293-300.

215 [3] Domenech O, Oliveira P. Transoesophageal echocardiography in the dog. Vet J
216 2013;198:329-38.

217 [5] Buchholz S, Jenni R. Doppler echocardiographic findings in 2 identical variants of a
218 rare cardiac anomaly, "subtotal" cor triatriatum: a critical review of the literature. J Am
219 Soc Echocardiogr 2001;14:846-9.

220 [6] Almeida G, Almeida M, Santos AC, Mattos A, Oliveira L, Braga R. Cor Triatriatum
221 Sinister in a French Bulldog. Hindawi Publishing Corporation 2012:1-4.

- 222 [7] Champion T, Gava FN, Garrido E, Galvão ALB, Camacho AA. Cor triatriatum sinister
223 and secondary pulmonary arterial hypertension in a dog. *Arq Bras Med Vet Zootec*
224 2014;66:310-14.
- 225 [8] Nassar PN, Hamdan RH. Cor Triatriatum Sinistrum: Classification and Imaging
226 Modalities. *Eur J Cardiovasc Med* 2011;1:84-7.
- 227 [9] Krabill KA, Lucas RV. Abnormal pulmonary venous connections. In: Emmanoulides
228 GC, Riemenschneider TA, Allen HD, Gutgesselle, editors. *Heart disease in infants,*
229 *children, and adolescents including the fetus and young adult.* 5th Ed. Baltimore:
230 Williams and Wilkins; 1995, p. 838-74.
- 231 [10] Patel MB, Samuel BP, Berjaoui WK, Girgis RE, Vettukattil JJ. Transcatheter
232 intervention in cor triatriatum sinister. *Can J Cardiol* 2015;31:819.e3-4.
- 233 [11] Johnson MS, Martin M, De Giovanni JV, Boswood A, Swift S. Management of cor
234 triatriatum dexter by balloon dilatation in three dogs. *J Small Anim Pract* 2004;45:16-20.
- 235 [12] Borenstein N, Gouni V, Behr L, Trehiou-Sechi E, Petit A, Misbach C, Raillard M,
236 Retortillo JL, Pouchelon JL, Pierrel A, Laborde F, Chetboul V. Surgical treatment of cor
237 triatriatum sinister in a cat under cardiopulmonary bypass. *Vet Surg* 2015;44:964-9.
- 238 [13] Keene BW and Tou SP. Cor triatriatum. In: Weisse C and Berent A. *Veterinary*
239 *image-guided interventions,* 1st Ed. Iowa: Wiley Blackwell; 2015, p. 604-9.
- 240 [14] Stern JA, Tou SP, Barker PC, Hill KD, Lodge AJ, Mathews KG, Keene BW. Hybrid
241 cutting balloon dilatation for treatment of cor triatriatum sinister in a cat. *J Vet Cardiol*
242 2013;15:205-10.

243

Figure legends

244 **Fig. 1:** Left lateral (A) and ventro-dorsal (B) thoracic radiographs from a French
245 Bulldog. Note the evidence of left atrial on lateral recumbency (A). The radiographic
246 border of the caudo-dorsal aspect of the left atrium is outlined (white dotted line) for a
247 better assessment of such radiographic change. No additional radiographic
248 abnormalities are evident.

249

250 **Fig. 2:** Two-dimensional transthoracic echocardiographic image obtained from a right
251 parasternal long axis view. Note the thin perforated membrane partitioning the left
252 atrium (LA) into two chambers: an accessory chamber and the true LA, which
253 includes the mitral valve annulus and the interatrial septum (A). Right parasternal
254 short axis view at the level of the cardiac base (B). Note that the accessory chamber
255 lays proximally to the left atrial appendage that is in direct continuation with the true
256 LA. In both views, some pulmonary veins drain into the true LA (white asterisks)
257 while other veins enter the accessory chamber (white stars). AC: accessory atrial
258 chamber; Ao: aorta; LA: left atrium; LV: left ventricle; RA: right atrium.

259

260 **Fig. 3: A.** Transesophageal echocardiographic view obtained with the probe placed
261 in middle position and showing a modified four-chamber view (A). Note the
262 fenestrated membrane (white star) dividing the left atrium from the accessory
263 chamber. Color Doppler analysis of the malformation from a left ventricular outflow
264 tract view (B). Note the continuous turbulent blood flow across the membrane's

265 orifice with a restrictive behavior and directed toward the anterior mitral valve leaflet.
 266 The numbers on top left of the images (141° and 116°) represent the degree of
 267 rotation of the crystal of the transesophageal probe. AC: accessory atrial chamber;
 268 Ao: aorta; LA: left atrium; LV: left ventricle; MV: mitral valve; RA: right atrium; RV:
 269 right ventricle; RVOT: right ventricular outflow tract.

270
 271 **Fig. 4: A.** Continuous-wave Doppler analysis of the transmembrane blood flow
 272 obtained from the same image as Figure 3B (A). Notice the continuous blood flow
 273 across the perforated membrane that is directed distally toward the left atrium. The
 274 minimal velocity is recorded during ventricular systole, while the maximal flow
 275 velocity across the membrane occurs during ventricular diastole, when the mitral
 276 valve is open. Color M-Mode analysis shows the distribution of the blood flow across
 277 the different left-sided chambers and their timing (B). The turbulent jet across the
 278 membrane invades the left atrium during the entire cardiac cycle, while the LV is
 279 filled normally during diastole. Mild mitral regurgitation is visualized in early systole
 280 as a thin red jet (arrowhead). AC: accessory atrial chamber; LA: left atrium; LV: left
 281 ventricle.

282

283 **Video Table**

Video	Title	Description

1	Transthoracic echocardiographic video clip obtained from a right parasternal long axis view in a French bulldog.	The left atrium is partitioned in two chambers, a proximal one (accessory chamber) and a true left atrium, which are divided by a perforated thin membrane. The pulmonary veins appear to drain partly into the accessory chamber and partly into the true left atrium. The other cardiac structures are normal. AC: accessory atrial chamber; LA: left atrium.
2	Color Doppler transthoracic echocardiographic video clip obtained from a left apical four-chamber view.	Note the hyperechoic band traversing the LA consistent with the anomalous membrane of <i>cor triatriatum sinister</i> (left panel). On color Doppler imaging (right panel), there is continuous flow arising from the membrane's orifice and directed toward the anterior mitral valve leaflet. Intermittent blood flow arising from some pulmonary veins that directly communicate with the true left atrial cavity is observed.
3	Color Doppler transesophageal	A continuous, turbulent blood flow

	echocardiographic video clip obtained from a left apical four-chamber view with visualization of the left ventricular outflow tract.	arising from the accessory atrial chamber and invading the true left atrium through the membrane orifice is evident. This flow is directed toward the anterior mitral valve leaflet. Note also the mild, eccentric, systolic blood flow across the mitral valve, consistent with mitral regurgitation.
--	--	--

